

Supplementary Information

**Transparent Electronic and Photoelectric Synaptic Transistors  
Based on the Combination of InGaZnO Channel and TaO<sub>x</sub> Gate  
Dielectric**

*Yuanbo Li,<sup>\*a</sup> Tupei Chen,<sup>a</sup> Xin Ju,<sup>\*a</sup> and Teddy Salim<sup>b</sup>*

1



Deposition: RF magnetron sputtering  
Patterning: No  
Process temperature: room temperature

2



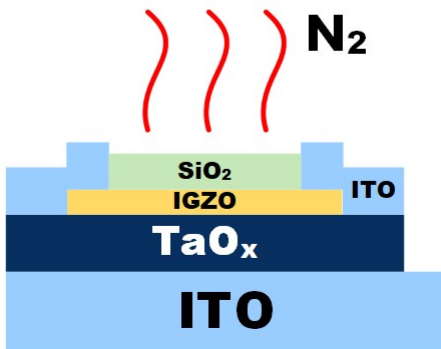
Deposition: RF magnetron sputtering  
Patterning: Lithography + Lift off  
Process temperature: room temperature

3



Deposition: RF magnetron sputtering  
Patterning: Lithography + Lift off  
Process temperature: room temperature

4



Deposition: Plasma enhanced chemical vapor deposition (PECVD)  
Patterning: Lithography + Reactive ion etch (RIE)  
Post-annealing: N<sub>2</sub> 300 °C 1 hour  
Process temperature: 300 °C

Fig. S1. Process flow of the synaptic IGZO TFT fabrication.

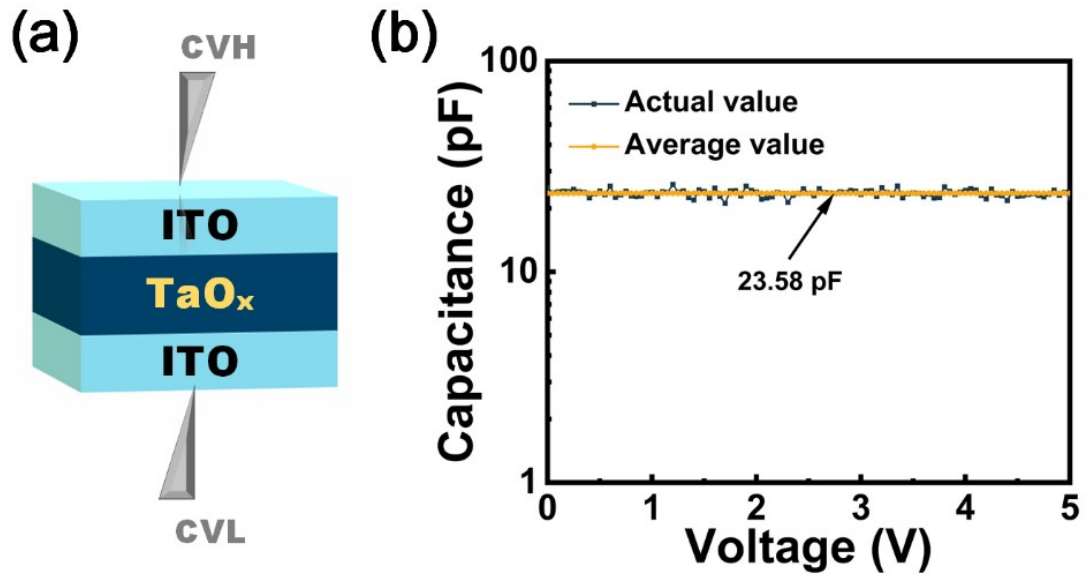


Fig. S2. (a) Schematic of the capacitor structure for C-V measurement. CVH and CVL are two probers for C-V measurement. (b) Result of the C-V measurement at 100k Hz of the TaO<sub>x</sub> layer with the thickness of 160 nm and effective area of 10<sup>4</sup> μm<sup>2</sup>.

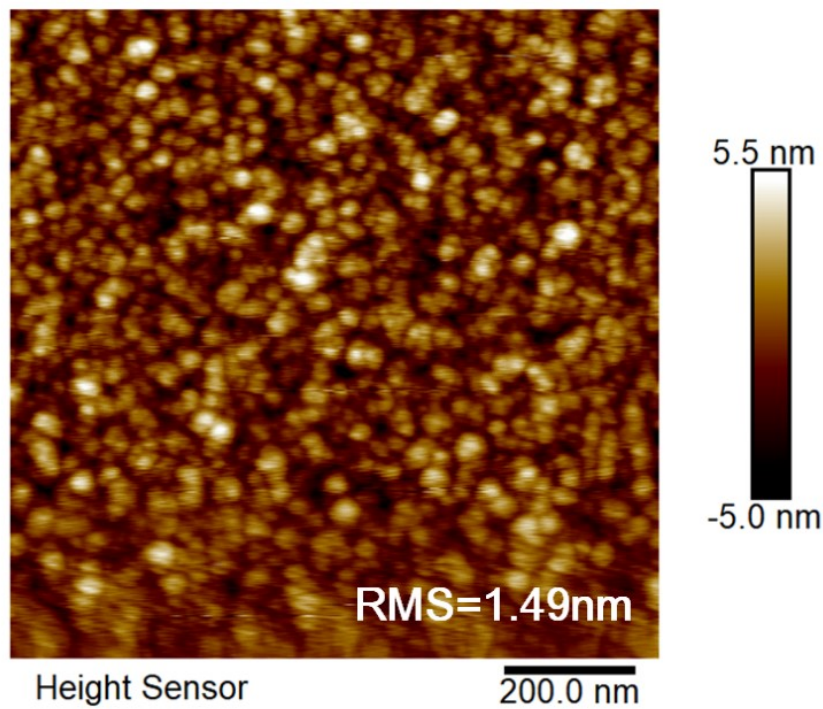


Fig. S3. 2D AFM image of the TaO<sub>x</sub> layer deposited by RF magnetron sputtering. The root mean square (RMS) of the roughness is 1.49 nm.

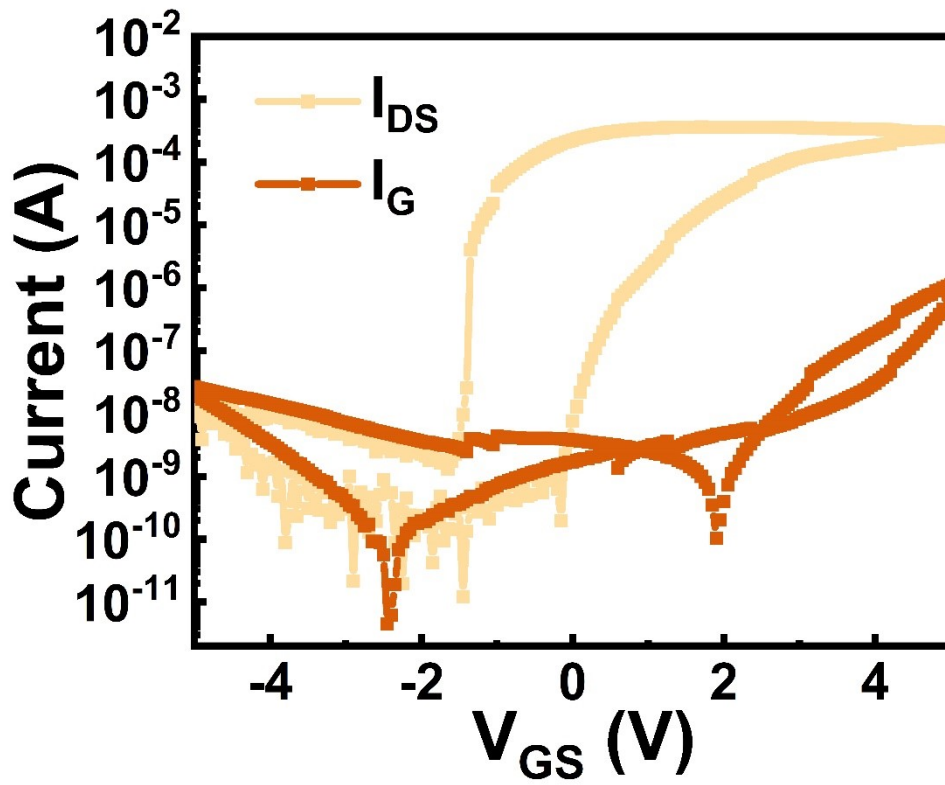


Fig. S4. Drain current  $I_{DS}$  and gate current  $I_G$  of the  $TaO_x$ -based IGZO TFT under DC sweep of the gate voltage from -5 V to 5V. The drain voltage was fixed at 0.5 V.

Table S1. Characteristics of the IGZO TFT

	Forward	Backward
Subthreshold swing (S.S.)	50 mV dec <sup>-1</sup>	150 mV dec <sup>-1</sup>
Threshold voltage ( $V_{TH}$ )	1.98 V	-1.25 V
$I_{on}/I_{off}$ ratio	$2.4 \times 10^7$	$2.8 \times 10^6$

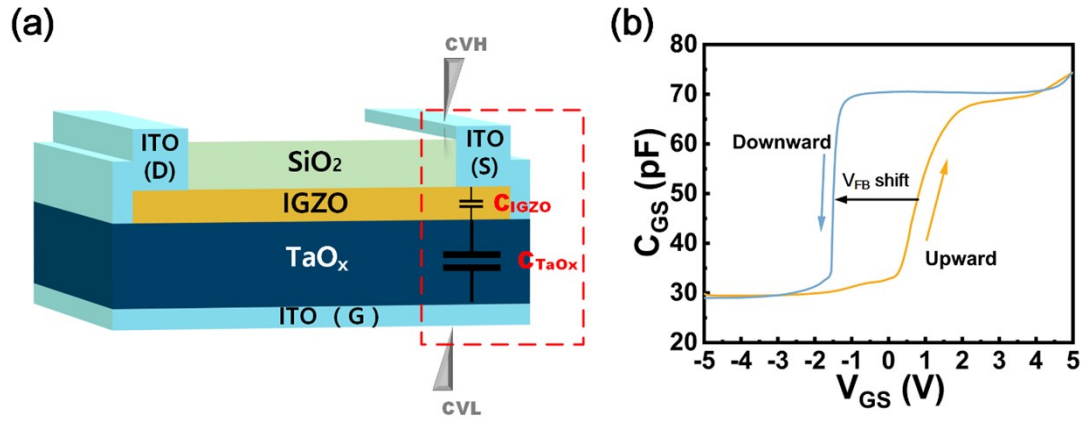


Fig. S5. (a) Schematic of the configuration of  $C_{GS}$  measurement. (b). Result of the  $C_{GS}$  measurement in the dual  $V_{GS}$  sweeps in the range of  $-5 \sim 5$  V. The  $V_{FB}$  shift was around 3 V, which could originate from the electrical charging inside the  $TaO_x$  layer.<sup>[35]</sup> Meanwhile, the slope of the C-V curve changed between the downward and upward  $V_{GS}$  sweep. The slope change could be attributed to the change of density of states (DOS) in the IGZO film.<sup>[36]</sup>

Table S2. Atomic concentration (%) of each species and O/Ta ratio in the  $TaO_x$  layer

Cycle	O <sub>L</sub>	O <sub>v</sub> /C-O	Ta <sup>4+</sup>	Ta <sup>3+</sup>	O/Ta ratio
0	58.02	10.19	31.79	-	1.825
1	64.66	3.71	31.34	0.29	2.162
2	64.27	4.14	29.73	1.86	2.166
3	63.95	4.33	29.52	2.21	2.152
4	63.42	4.71	29.00	2.87	2.138
5	62.23	5.86	28.86	3.05	2.134
6	62.08	6.13	28.06	3.73	2.146
7	60.78	6.57	27.71	4.94	2.063

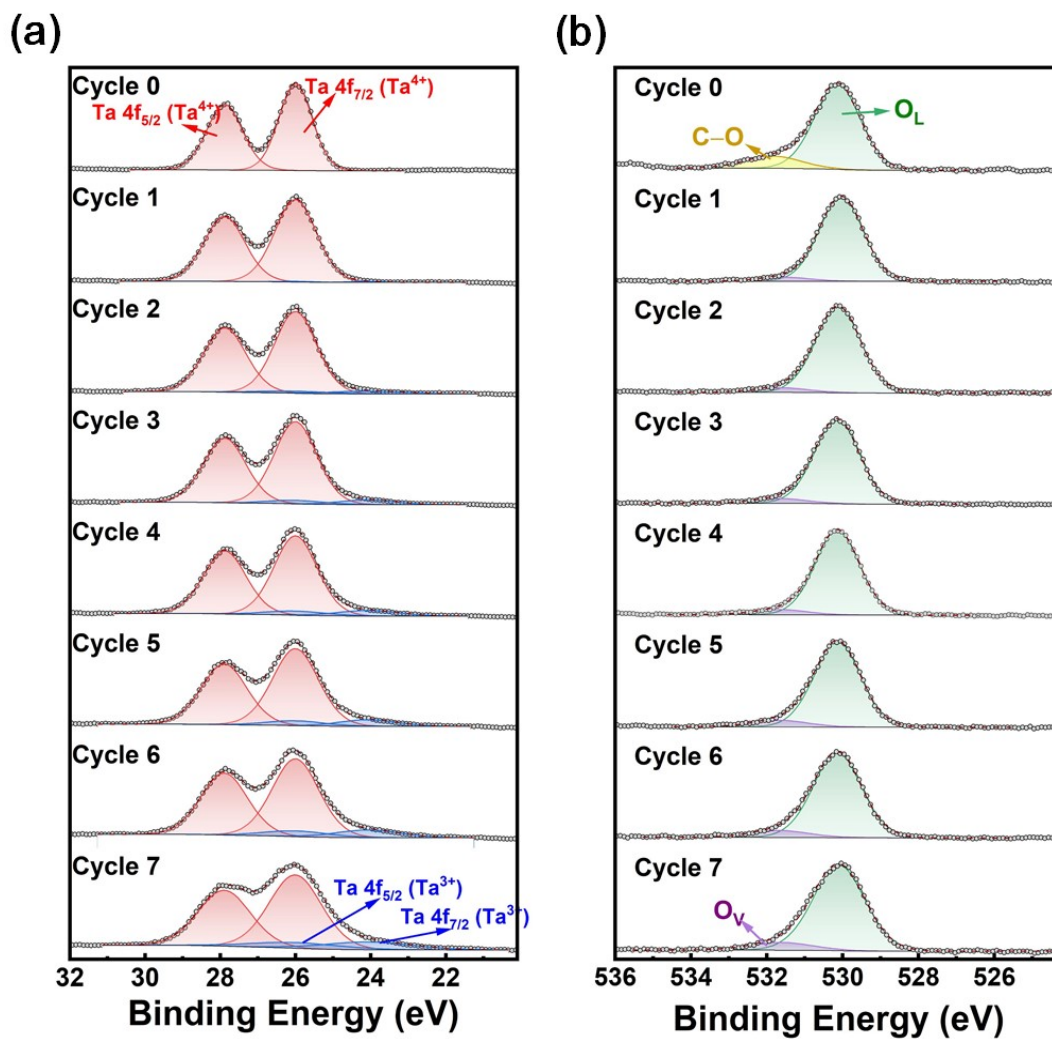


Fig. S6. (a) Ta 4f spectra and (b) O 1s spectra of the surface region of the TaO<sub>x</sub> layer obtained after various etching cycles. The C-O peak at the ‘cycle 0’ of O 1s spectra could be due to some organic bonding at the surface.

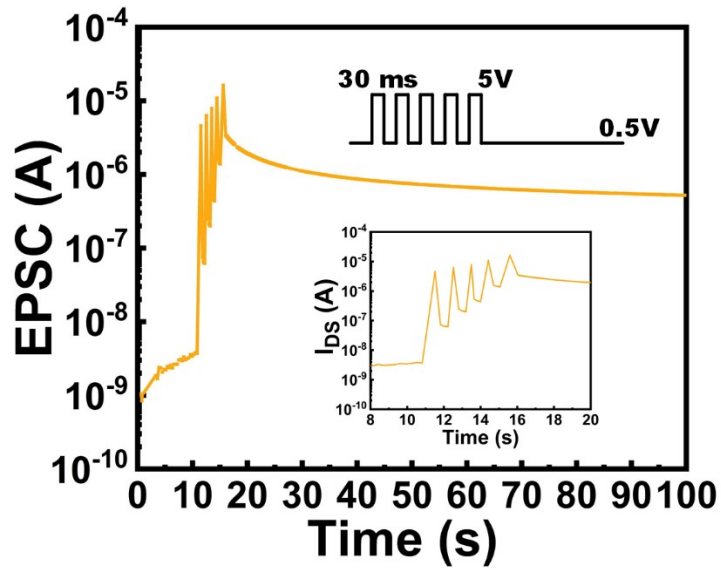


Fig. S7. EPSC of the TFT under stimulation of 5 consecutive voltage pulses with pulse width of 30 ms, amplitude of 5 V and base level of 0.5V. The inset is the zoom-in region of the EPSC under 5 voltage pulses.

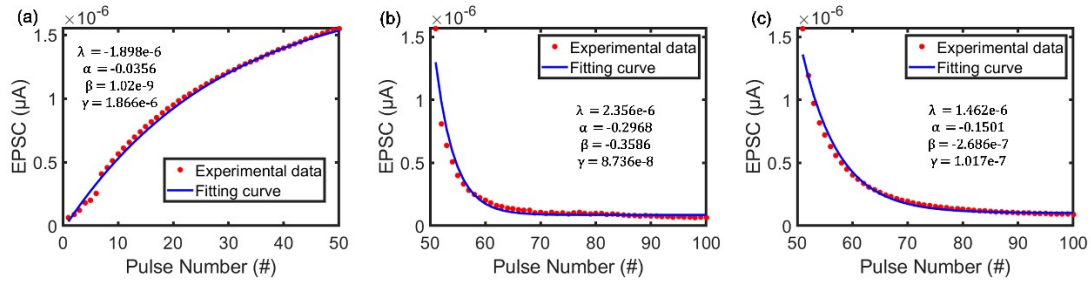


Fig. S8. Fittings to the experimental data of (a) the potentiation under 50 consecutive positive pulses with amplitude of 1.8 V, pulse width of 30 ms, and base level of 0.1 V, (b) the depression under 50 consecutive negative pulses with amplitude of -1 V, pulse width of 30 ms, and base level of 0.1 V, and (c) the depression under 50 consecutive negative pulses with step-increasing amplitudes (0.05 V ~ 1.2 V), pulse width of 30 ms, and base level of 0.1 V.

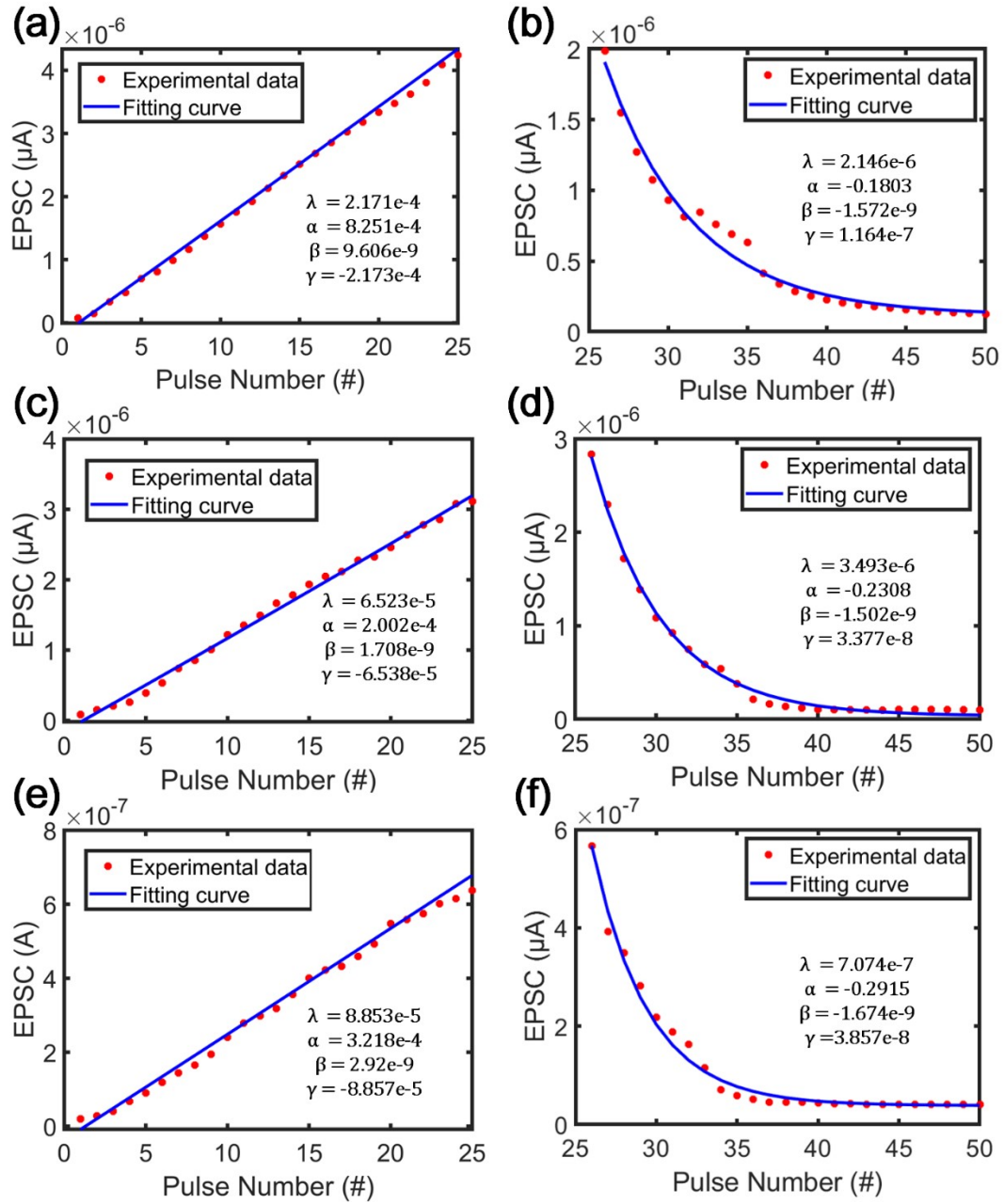


Fig. S9. Fitting results of the non-linearity of (a) the potentiation under 25 consecutive UV light pulses and the base level of 0.1 V; (b) the depression under 25 consecutive negative voltage pulses with increasing amplitudes (0.5 V ~ 1.2 V) and base level of 0.1 V; (c) the potentiation under 25 consecutive blue light pulses and the base level of 0.1 V; (d) the depression under 25 consecutive negative voltage pulses with increasing amplitudes (0.05 V ~ 1 V) and base level of 0.1 V; (e) the potentiation under 25 consecutive green light pulses and the base level of 0.1 V; (f) the depression under 25 consecutive negative voltage pulses with increasing amplitudes (0.05 V~1 V) and base level of 0.1 V.



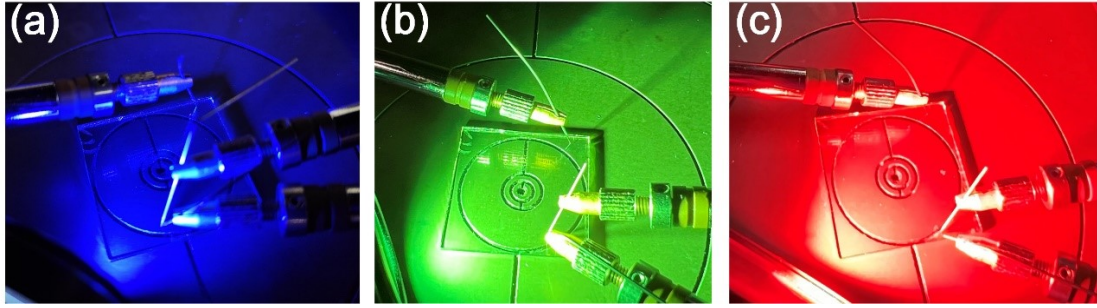


Fig. S10. Photos of the experimental setup under the illumination of blue light (a), green light (b) and red light (c). The wavelengths of the blue light, green light and red light were 470 nm, 525 nm, and 633 nm, respectively.

Table S3. Comparison of P/D characteristics among different stimulation schemes

External pulse	#	$G_{\max}/G_{\min}$	$ \alpha_p $	$ \alpha_D $	$  \alpha_p  -  \alpha_D  $	Endurance
Electronic	50	24.9	$3.56 \times 10^{-2}$	0.1501	0.1145	Good
UV-photoelectric	25	55	$8.251 \times 10^{-4}$	0.1803	0.1795	Good
Blue-photoelectric	25	36.6	$2.002 \times 10^{-4}$	0.2308	0.2306	Fair
Green-photoelectric	25	31.6	$3.218 \times 10^{-4}$	0.2916	0.2913	Poor

Note: # refers to the pulse number;  $||\alpha_p| - |\alpha_D||$  refers to the asymmetry.

### Results of the IGZO TFTs based on SiO<sub>x</sub>

The oxygen vacancies can be provided from other oxide dielectric layer such as SiO<sub>x</sub>, AlO<sub>x</sub>, HfO<sub>x</sub>, etc. Among these oxides, we choose SiO<sub>x</sub> for the study of comparison. The reasons are as follows: 1). HfO<sub>x</sub> concurrently owns different characteristics, including ferroelectricity, charge-

trapping effects, and ion-conductivity. The present study is on the synaptic behaviors of the TFT resulting from ion-conductivity. Therefore,  $\text{HfO}_x$  is not considered here to exclude the influence of those non-ion-conductivity characteristics. 2).  $\text{AlO}_x$  can be deposited by RF sputtering with  $\text{Al}_2\text{O}_3$  ceramic target. However, the deposition rate is ultra-slow. It is time consuming and thus not ideal to choose  $\text{AlO}_x$  as the dielectric layer for synaptic TFT. 3).  $\text{SiO}_x$  is feasible by sputtering with  $\text{SiO}_2$  ceramic target with a reasonable deposition rate.  $\text{SiO}_x$  doesn't have significant interfering variables. The  $\text{SiO}_x$ -based IGZO TFT had nearly the same fabrication process as the  $\text{TaO}_x$ -based IGZO TFT.

The  $\text{SiO}_x$ -based TFT showed much inferior electrical characteristics compared with the  $\text{TaO}_x$ -based TFT. Fig. S11 shows the transfer curves of the  $\text{SiO}_x$ -based IGZO TFT. The S.S. was much deteriorated compared with that of the  $\text{TaO}_x$ -based IGZO TFT. The deteriorated S.S. could be attributed to smaller oxide capacitance as a result of much lower dielectric constant and poor interface quality (i.e., more trap states). The on-current of the  $\text{SiO}_x$ -based IGZO TFT was much lower as compared with the  $\text{TaO}_x$ -based IGZO TFT, which could be originated from the low dielectric constant of the  $\text{SiO}_x$  layer. Fig. S12 shows the EPSC of the  $\text{SiO}_x$ -based IGZO TFT under the stimulation of 5 consecutive gate voltage pulses with the base level of 0.1 V, pulse width of 30 ms and amplitudes increasing from 5 to 8 V. Only when the pulse amplitude exceeded 7 V, could the EPSC behavior be stimulated. Still, the EPSC decayed fast in 10 seconds even under the pulses with the amplitude of 8 V. Obviously, the  $\text{SiO}_x$ -based IGZO TFT showed weaker synaptic behaviors as compared with the  $\text{TaO}_x$ -based IGZO TFT.

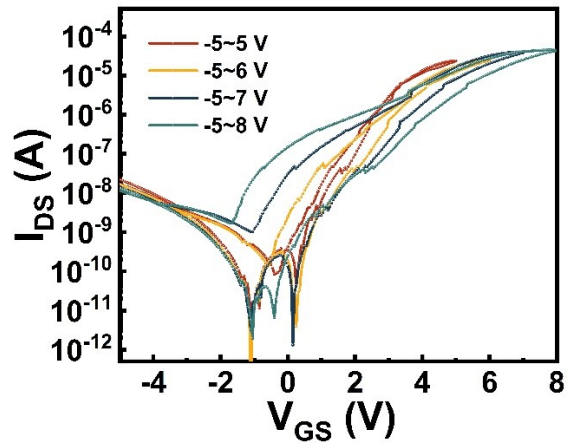


Fig. S11. Transfer curves of the  $\text{SiO}_x$ -based IGZO TFT under the drain voltage of 0.5 V.

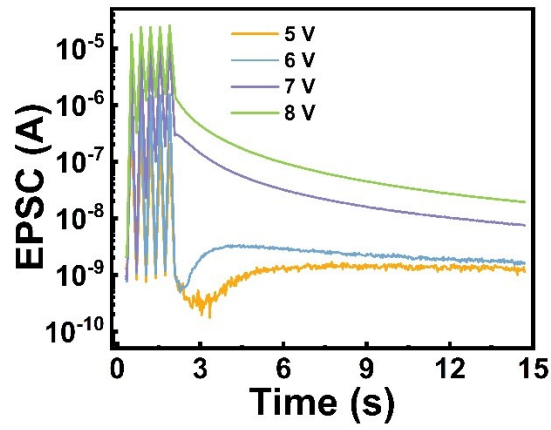


Fig. S12. EPSC of the  $\text{SiO}_x$ -based IGZO TFT under the stimulation of 5 consecutive gate voltage pulses with the base level of 0.1 V, pulse width of 30 ms and amplitudes increasing from 5 to 8 V.